Spin Current for Spin-Orbit Torque in Magnetoresistance Structure

Sena Kobayashi,[1] Yoshikazu Yamaki,[1] Syuta Honda,[1*] and Hiroyoshi Itoh[1]

(Received September 8, 2023; accepted January 11, 2024)

Abstract:

The magnetization of ferromagnetic metal can be reversed by spin-orbit torque, a principle used in spintronic devices such as magnetoresistive random access memory. To increase this torque, the injected spins from heavy metals must significantly diffuse into the ferromagnetic metal. However, the thin nature of ferromagnetic metal often leads to the passage of injected spins through it. We analyzed the spin current in a magnetic junction composed of a heavy metal/ferromagnetic metal/non-magnetic layer/ferromagnetic pinned layer/non-magnetic lead. Spin diffusion within the ferromagnetic metal increases with the decreasing conductivity of the non-magnetic material, increasing thickness of the non-magnetic layer, and decreasing thickness of the ferromagnetic pinned layer. These findings are expected to contribute to the advancement of spintronic devices such as spin-orbit torque magnetoresistive random-access memory.

1 Introduction

Spin-orbit torque (SOT), a type of spin-transfer torque, plays a pivotal role in influencing the magnetization of a ferromagnetic metal (FM). This phenomenon commonly occurs in FM structures layered atop a heavy metal (HM), as depicted in Fig. 1[1),2)]. By passing current through the HM, the trajectory of charge carriers can be manipulated. For example, when carrier electrons move in the (1, 0, 0) direction, electrons with spins polarized in the (0, 1, 0) direction are redirected towards (0, 0, 1). In contrast, electrons with spins polarized in the (0, −1, 0) direction deviate from their original trajectory and shift towards (0, 0, −1). This scientific phenomenon is known as the spin-Hall effect (SHE)[3),4),5)].

When an FM is stacked on top of a HM, the spin deviated toward the FM is injected into the FM. These injected spins diffuse within the FM, exerting torque on the magnetization of the FM and resulting in magnetization reversal[6),7)]. The time variation of the magnetization of the FM is described by

$$\frac{\partial \boldsymbol{m}}{\partial t} = -\frac{|\gamma|}{M_s}\mathrm{div}\boldsymbol{S}, \tag{1}$$

where $\boldsymbol{m}$ is a unit vector of a magnetic moment, t is time, γ is the gyro magnetic ratio, M_s is a saturated magnetization of the FM, and $\boldsymbol{S}$ is a spin current density tensor. The magnitude of div$\boldsymbol{S}$ corresponds to the amount of spin current diffused in the FM. The greater the diffusion of the spin current, the greater the change in magnetization of the FM. Specifically, the spin

1 Department of Pure and Applied Physics, Kansai University, Suita, Osaka 564-8680, Japan
* Correspondence to: Syuta Honda, Department of Pure and Applied Physics, Kansai University, Suita, Osaka 564-8680, Japan. E-mail: shonda@kansai-u.ac.jp

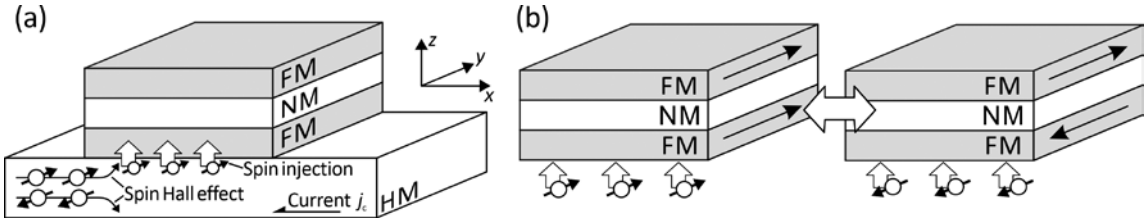

Fig. 1. Schematic of (a) a spin injection via a spin-Hall effect of the HM layer in an HM/FM/NM/FM junction and (b) a magnetization reversal due to the spin injection. The long arrows shown in two FM layers in (b) represent the magnetization direction.

current flowing from the HM into the FM is a crucial parameter influencing the magnetization dynamics of the FM.

We have analytically solved for the spin current, $\boldsymbol{S}$, in the HM/FM junction incorporating the SHE[8]. In our analytical calculations, we introduced the spin flow due to the SHE as a pseudopotential. For example, when the thicknesses of the HM and FM layers significantly exceed their respective spin diffusion lengths, the magnitude of the spin current density at the junction interface, $j_{\mathrm{spin}}^{\mathrm{inter}}$, which is the spin current density injected into the FM, can be calculated as

$$j_{\mathrm{spin}}^{\mathrm{inter}} = \frac{\hbar}{2}\frac{\lambda_{\mathrm{HM}}\sigma_{\mathrm{FM}}}{\lambda_{\mathrm{HM}}\sigma_{\mathrm{FM}} + \lambda_{\mathrm{FM}}\sigma_{\mathrm{HM}}}\frac{\theta_{\mathrm{SH}} j_{\mathrm{c}}}{q}. \tag{2}$$

Furthermore, the spin current density decays exponentially within the FM, as shown in

$$j_{\mathrm{spin}}^{\mathrm{FM}}(z) = j_{\mathrm{spin}}^{\mathrm{inter}} \exp\left(-\frac{z}{\lambda_{\mathrm{FM}}}\right). \tag{3}$$

Here, λ_{HM} and λ_{FM} represent the spin-diffusion length in the HM and FM, respectively. σ_{HM} and σ_{FM} denote the conductivity of carriers in the HM and FM, respectively, while θ_{SH} is the spin-Hall angle of the carrier in the HM. j_{c} corresponds to the current flowing parallel to the interface in the HM, q is the charge of the carrier ($q < 0$), and $\hbar$ is the Dirac constant (reduced Planck constant). The variable z represents the distance from the interface between the HM and the FM.

Both the spin diffusion length and electrical conductivity are assumed to be independent of spin. Equation (2) is commonly used as the spin current density injected into the FM when analyzing the magnetization reversal by the SOT, with the second coefficient approximated by 1, represented as $\frac{\hbar}{2}\frac{\theta_{\mathrm{SH}} j_{\mathrm{c}}}{q}$. However, in the case of thin FM layers used in magnetoresistive random-access memory (MRAM), the spin injection density $j_{\mathrm{spin}}^{\mathrm{inter}}$ is smaller than that of the original equation (2).

When the HM and/or FM are thin, $j_{\mathrm{spin}}^{\mathrm{FM}}$ is described by a more complex equation[8]. In devices that perform spin injection and magnetization reversal, such as magnetic resistance elements, the FM is typically thin. In addition, on the opposite side of the FM (FM_2), there exists another FM (FM_2) connected by a non-magnetic (NM) layer, creating a structure known as an HM/FM_1/NM layer/FM_2/NM lead structure. This serves as a basic structure for SOT-MRAM. The magnetization of the first FM (FM_1) is free, while that of the second FM (FM_2) is pinned. SOT switches the magnetization of FM_1. The thickness of FM_1 is on the

order of a few nanometers. Given that this thickness is similar to the spin diffusion length for FM_1, the spins injected into FM_1 from the HM can flow into the NM layer side without significant spin diffusion occurring within FM_2. Insufficient spin diffusion within FM_1 may impede magnetization reversal.

We investigate the relationship between the properties of the NM layer, FM_2, their thicknesses, and the spin current that undergoes spin diffusion within FM_1. The complexity of analyzing the spin current in this structure increases when using equations. Therefore, in this study, numerical analysis is employed to analyze the spin current in the HM/FM_1/NM layer/FM_2/NM lead structure.

2 Model and Method

The spin current is determined by utilizing the continuity equation for spin-dependent currents. Since the spin current is the difference between the flow of spin-up and spin-down, our calculations focus on determining this difference without individually calculating the flow or quantity of each spin. We focus on a layered structure of HM/FM_1/NM layer/FM_2/NM lead, characterized by finite thicknesses and infinite planes. We assume that each layer represents an infinite plane parallel to the x-y plane, with a current flowing in the $-x$-direction. Due to the SHE within the HM, spins polarized in the $+y$-direction ($-y$-direction) are bent in the z-direction ($-z$-direction). As not all variables depend on the x- or y-position, we utilize a one-dimensional model along the z-direction.

A continuity equation of the density of the spin-up of the carrier ($n_\uparrow$) is given as

$$\frac{dn_\uparrow}{dt} = -\frac{1}{q}\frac{dj_\uparrow}{dz} - \frac{n_\uparrow}{2\tau_{\uparrow 0}} + \frac{n_\downarrow}{2\tau_{\downarrow 0}} \tag{4}$$

and that of the spin-down of the carrier ($n_\downarrow$) is given as

$$\frac{dn_\downarrow}{dt} = -\frac{1}{q}\frac{dj_\downarrow}{dz} - \frac{n_\downarrow}{2\tau_{\downarrow 0}} + \frac{n_\uparrow}{2\tau_{\uparrow 0}}, \tag{5}$$

where t represents time, q denotes the electron charge of -1.6×10^{-19} C, and $j_{\uparrow(\downarrow)}$ corresponds to the spin-resolved current densities of the spin-up (down) along the y-direction. $\tau_{\uparrow(\downarrow)0}$ represents the spin relaxation times of spin-up (down). The spin-resolved current densities $j_{\uparrow(\downarrow)}$ are given as

$$j_\uparrow = \sigma_\uparrow E_z - qD_\uparrow \frac{\partial n_\uparrow}{\partial z} - \theta_{\mathrm{SH}} \frac{n_\uparrow}{n_\uparrow + n_\downarrow} j_c \tag{6}$$

and

$$j_\downarrow = \sigma_\downarrow E_z - qD_\downarrow \frac{\partial n_\downarrow}{\partial z} + \theta_{\mathrm{SH}} \frac{n_\downarrow}{n_\uparrow + n_\downarrow} j_c, \tag{7}$$

where $\sigma_{\uparrow(\downarrow)}$ is the conductivity of each spin, E_z is an electric field along the z-direction, $D_{\uparrow(\downarrow)}$ is the diffusion coefficient of each spin, θ_{SH} is the spin Hall constant, and j_c is the density of the current along the $-x$-direction. The spin current is calculated using these equations and boundary conditions.

In the HM, NM layer, and NM lead, the spin relaxation time is spin-independent ($\tau_{\uparrow 0} = \tau_{\downarrow 0}$). In contrast, the spin relaxation time usually depends on the spin in the FM ($\tau_{\uparrow 0} \neq \tau_{\downarrow 0}$). We assume that τ does not depend on the spin of the FM ($\tau_{\uparrow 0} = \tau_{\downarrow 0} = \tau$). The spin Hall

constant θ_{SH} is $\theta_{SH} \neq 0$ in HM, while $\theta_{SH} = 0$ in FM_1, FM_2, NM layer, and NM lead. We assume that the conductivity $\sigma_{\uparrow(\downarrow)}$ and the diffusion coefficient $D_{\uparrow(\downarrow)}$ are spin-independent ($\sigma_\uparrow = \sigma_\downarrow = \sigma$, $D_\uparrow = D_\downarrow = D$), and that the current density j_c does not depend on the z-position in the HM. Under the steady state ($dj_s/dt = 0$), the spin current density j_s becomes

$$j_s = \frac{\hbar}{2}\frac{1}{q}\left(j_\uparrow - j_\downarrow\right) = \frac{\hbar}{2}\frac{1}{q}\left(-qD\frac{\partial}{\partial z}(n_\uparrow - n_\downarrow) - \theta_{SH} j_c\right) = \frac{\hbar}{2}\frac{1}{q}\left(-\frac{\sigma}{q}\frac{\partial \delta\mu}{\partial z}\right), \tag{8}$$

where $\delta\mu$ is a difference of a spin-resolved electrochemical potential including the SHE[8] of

$$\delta\mu = k_B T\frac{n_\uparrow}{n_{\uparrow 0}} - k_B T\frac{n_\downarrow}{n_{\downarrow 0}} + \frac{q}{\sigma}\theta_{SH} j_c z \tag{9}$$

and D is the electrical mobility equation (Einstein relation) of $D = \frac{\mu_q k_B T}{q} = \frac{\sigma k_B T}{q^2 n_0}$, where μ_q represents electron mobility, k_B represents the Boltzmann constant, T represents temperature, and n_0 represents the density of each carrier. Moreover, the spin diffusion length λ is defined as $\lambda = (D\tau)^{1/2}$. We neglect spin-dependent interface resistance and spin scattering at each surface and interface, even though these effects can significantly impact conduction carriers. For example, one source contributing to the giant magnetoresistance effect is the spin-dependent resistance occurring at the interface[5]. In this study, however, we intentionally ignore these effects to focus on analyzing the impact of each layer on the spin current. The boundary conditions at each surface and interface are as follows: the spin current j_s is zero at each surface, $\delta\mu$ is zero at each surface, the spin current j_s of two adjacent layers is equal at each interface, and $\delta\mu$ of two adjacent layers is equal at each interface[8]. Solving equations (8) and (9) in accordance with these boundary conditions yields the spin current j_s.

The following parameters were used: the spin diffusion length of the HM was $\lambda_{HM} = 1$ nm, electrical conductivity was $\sigma_{HM} = 1.0 \times 10^7$ A/V/m, and the spin-Hall angle was $\theta_{SH} = 0.1$, assumed to be Pt. The current density flowing through the HM was $j_c = 1.0 \times 10^{10}$ A/m^2. The maximum value of the spin current in the HM was defined as j_{sHM} when the HM thickness was long. j_{sHM} is $\frac{\hbar}{2}\frac{1}{q}\theta_{SH} j_c$. The spin diffusion lengths of both FMs were set to $\lambda_{FM} = 2$ nm, and the conductivity $\sigma_{FM} = 1.0\ \sigma_{HM} = 1.0 \times 10^7$ A/V/m, assumed to be Fe. The spin diffusion length of NM lead was set to $\lambda_{NM\text{-}lead} = 200$ nm, and its conductivity was set at $\sigma_{NM\text{-}lead} = 6.0\ \sigma_{HM} = 6.0 \times 10_7$ A/V/m, assumed to be Cu. The thickness of the NM lead was specified as 10 nm. In addition, the temperature was set to $T = 300$ K, and the spatial discretization in the numerical calculations was set to $\delta d = 0.01$ nm.

3 Calculation results and discussion

The spin current was calculated in the 5-nm-HM/1-nm-FM_1/NM layer/5-nm-FM_2/10-nm-NM lead configuration. First, calculations were performed assuming an NM metal with high conductivity and a long spin diffusion length as the NM layer. The spin diffusion length was set to 200 nm for both the NM layer and the NM lead, and the conductivity was assumed to be $\sigma_{NM} = 6.0\sigma_{HM} = 6.0 \times 10^7$ A/V/m, assuming Cu.

Figure 2(a) shows the computed spin current j_s at the junction with the NM metal thicknesses of 1.0 nm, 2.5 nm, and 5.0 nm. The spin currents in the HM were generated through the SHE and reached a peak value of 0.86 j_s / j_{sHM} with little dependence on the

thickness of the NM metal. As the spin current decreased towards the HM/FM_1 interface, it successfully entered FM_1. At the interface of the HM/FM_1, the spin current measured approximately $0.30j_s$ / j_{sHM} without being significantly affected by the thickness of the NM metal. In FM_1, the spin current exhibited a linear decrease. However, the spin current did not reach zero on the opposite side of FM_1 (z = 1.0 nm). The spin current was continuously injected into the NM metal, remaining constant without any attenuation.

The spin current flowing through the NM metal entered FM_2 and decayed exponentially until it reached zero at the FM_2/NM-lead interface. The diffusion of spin within FM_1, denoted as Δj_s and indicating the difference between spin currents at the HM/FM_1 interface and the FM_1/NM layer interface, is affected by the thickness of the NM metal. Figure 2(b) illustrates the dependence of Δj_s on the NM metal thickness, showing a monotonic increase with the thickness of the NM metal. Increasing the thickness of FM_1 from 1.0 nm to 10.0 nm resulted in an approximately 11% increase in Δj_s.

Next, we examined an NM insulator with high resistance and a long spin diffusion length as the NM layer. The spin diffusion length was set to 200 nm, with an electrical conductivity of $\sigma_{NM} = 0.01\sigma_{HM} = 0.01 \times 10^7$ A/V/m. Figure 3(a) shows the computed spin current j_s for junctions with NM insulator thicknesses of 1.0 nm, 2.5 nm, and 5.0 nm. The peak of the generated spin current within the HM was 0.86 j_s/j_{sHM}, comparable to the junction with the NM metal. The spin current was injected into FM_1, decreasing linearly and approaching zero at the FM_1/NM insulator interface (z = 1.0 nm).

Figure 3(b) shows the relationship between Δj_s and the NM insulator thickness. Δj_s increased with increasing thickness of the NM insulator, but its increase was only a few percent for NM thickness of a few nanometers. When the NM insulator thickness was 3 nm or greater, Δj_s hardly increased because the spin current scarcely flowed through the NM insulator.

When the NM layer functioned as the insulator, the spin current j_s at the HM/FM interface (z = 0) decreased compared to the case when the NM layer functioned as the metal, as depicted in Fig. 2(a). This reduction occurred due to the reflection of the spin current at the interface of the FM/NM layer and its return to the HM side. Although there is spin diffusion

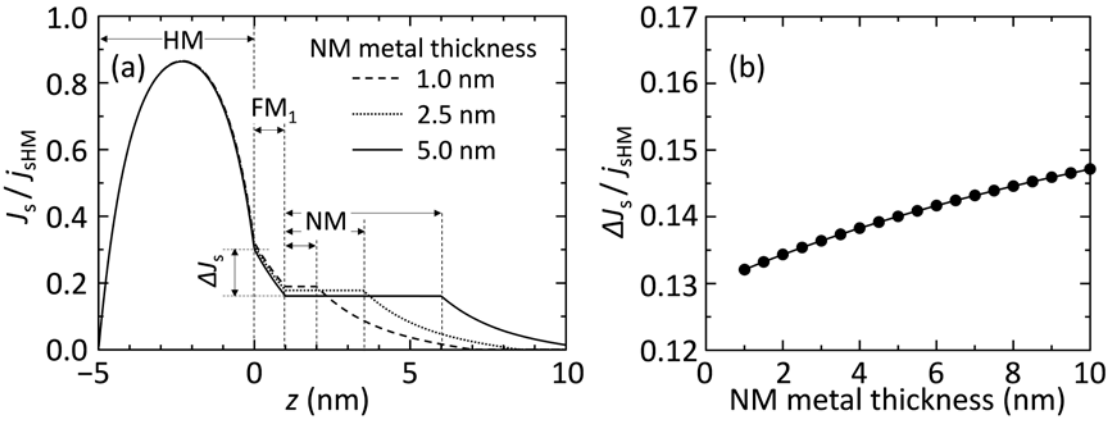

Fig. 2. The dependence of (a) the spin current and (b) the spin diffusion within FM_1 in 5-nm-HM/1-nm-FM_1/NM metal/5-nm-FM_2/10-nm-NM lead junctions on NM metal thickness.

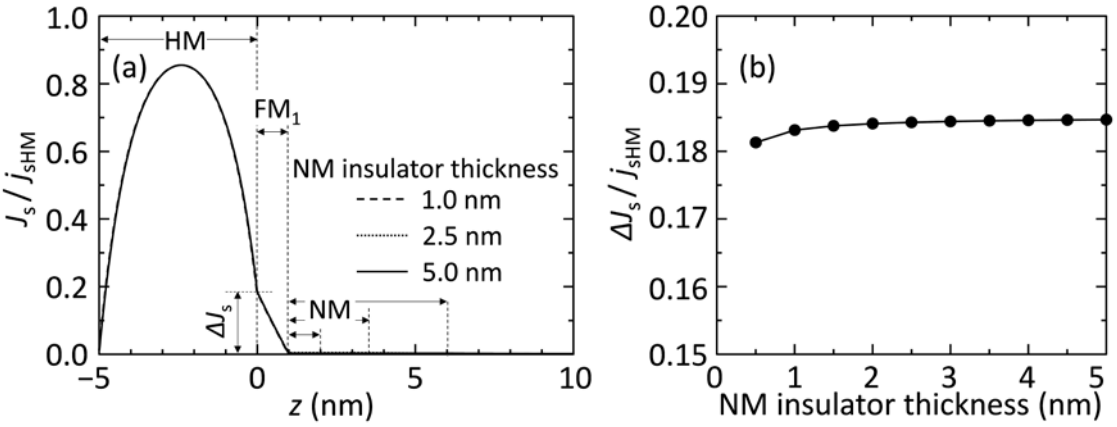

Fig. 3. The dependence of (a) the spin current and (b) the spin diffusion within FM_1 in 5-nm-HM/1-nm-FM_1/NM insulator/5-nm-FM2/10-nm-NM lead junctions on NM insulator thickness.

during the backflow, the amount of spin diffusion within the FM is more significant in the NM insulator compared to the NM metal.

Figure 4 illustrates Δj_s based on the conductivity of the NM layer in junctions with NM layer thicknesses of 1.0 nm and 2.0 nm. Δj_s increased with decreasing conductivity of the NM layer. As σ decreased, $\Delta j_s/j_{sHM}$ approached 0.184, while as σ increased, $\Delta j_s/j_{sHM}$ approached 0.132. When $\Delta j_s/j_{sHM}$ was between those two values, $\Delta j_s/j_{sHM}$ for the junction with the NM layer thickness of 2.0 nm was larger than that with the NM layer thickness of 1.0 nm.

Finally, we examined the spin current dependence on the FM_2 thickness in the junction with the NM metal. Figure 5(a) displays the computed spin current j_s for junctions with FM_2 thicknesses of 1.0 nm, 2.5 nm, and 5.0 nm. The behaviors of spin currents in FM_1 and NM metal were found to be consistent with the calculated results presented in Fig. 2. The spin current in FM_2 decayed almost linearly in the junction with the FM_2 thickness of 1.0 nm

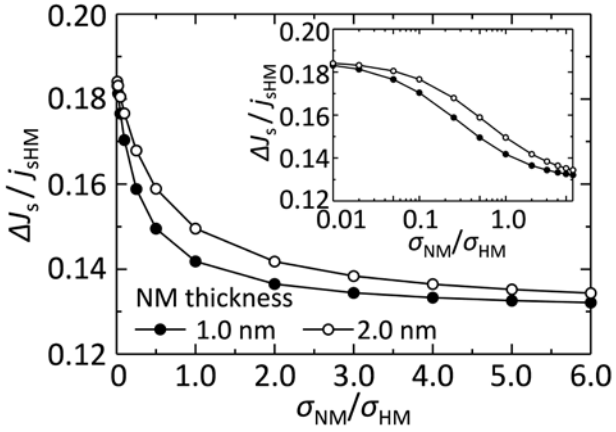

Fig. 4. The dependence of spin current diffusion within the FM_1 layer of the 5-nm-HM/ 1-nm-FM_1/ NM layer/5-nm-FM_2/10-nm-NM lead junctions on the conductivity σ_{NM} of the NM layer with 1.0 nm thickness and 2.0 nm thickness.

because the FM_2 thickness was shorter than the spin diffusion length in FM_2. Furthermore, the calculated values of the spin current in FM_1 and NM metal in the junction with an FM_2 thickness of 1.0 nm were smaller than those for an FM_2 thickness of 5.0 nm. The spin current in FM_1 and NM metal in the junction with an FM_2 thickness of 2.5 nm was intermediate compared to the values for FM_2 thicknesses of 1.0 nm and 5.0 nm. Figure 5(b) shows the dependence of Δj_s on the FM_2 thickness. Δj_s decreased with increasing thickness of the FM_2. Increasing the thickness of FM_2 from 1.0 nm to 3.0 nm resulted in an approximately 12% decrease in Δj_s. Most of the spin current injected from the HM into FM_1 diffuses through FM_1 and FM_2. As the length of FM_2 increased, the amount of spin current that diffuses through FM_2 also increased, while the amount of the diffusion of spin within FM_1 Δj_s decreased. Fortunately, additional increases in FM_2 thickness above 3.0 nm had minimal effect on decreasing Δj_s.

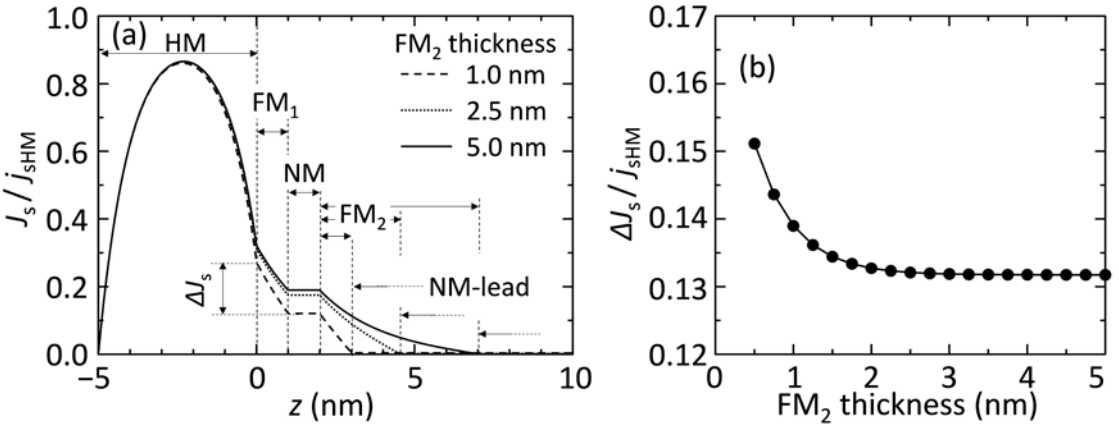

Fig. 5. The dependence of (a) the spin current and (b) the spin diffusion within FM_1 in 5-nm-HM/1-nm-FM_1/1-nm-NM layer/FM_2/10-nm-NM lead junctions on FM_2 thickness.

4 Conclusion

We investigated the diffusion of the spin current in FM_1 (free layer) resulting from the injection of spin current from the HM into FM_1 within the HM/FM_1/NM layer/FM_2 (pinned layer)/NM lead junction. The spin current was numerically calculated using a spin-dependent drift-diffusion method that incorporated the pseudopotential for the SHE. The amount of spin diffusion in FM_1 increased with a decrease in the conductivity of the NM layer, an increase in the thickness of the NM layer, and a decrease in the thickness of the FM_2. The variation in the amount of spin diffusion reached approximately 50%. These findings are expected to contribute to the advancement of spintronic devices such as SOT-MRAM.

Acknowledgments

This study was supported by CREST, the Japan Science and Technology Agency (Grant Number JPMJCR21C1), and the Japan Society for the Promotion of Science KAKENHI (Grant Number 20H02607, 23K17765, and 23H01438).

References

1) C. Zhang, S. Fukami, H. Sato, F. Matsukura, and H. Ohno, Spin-orbit torque induced magnetization switching in nano-scale Ta/CoFeB/MgO, *Applied Physics Letters*, **107**, 012401 (2015).
2) C. Song, R. Zhang, L. Liao, Y. Zhou, X. Zhou, R. Chen, Y. You, X. Chen, and F. Pan, Spin-orbit torques: Materials, mechanisms, performances, and potential applications, *Progress in Materials Science*, **118**, 100761 (2021).
3) J. E. Hirsch, Spin Hall Effect, *Physical Review Letters*, **83**, 1834-1837 (1999).
4) T. Jungwirth, J. Wunderlich, and K. Olejn?k, Spin Hall effect devices, *Nature Materials*, **11**, 382-390 (2012).
5) S. Bhatti, R. Sbiaa, A. Hirohata, H. Ohno, S. Fukami, S. N. Piramanayagam, Spintronics based random access memory: A review, *materials today*, **20**, 530-548 (2017).
6) J. C. Slonczewski, Current-driven excitation of magnetic multilayers, Journal of *Magnetism and Magnetic Materials*, **159**, L1-L7 (1996).
7) L. Berger, Emission of spin waves by a magnetic multilayer traversed by a current, *Physical Review B*, **54**, 9353 (1996).
8) Y. Yamaki, S. Honda, and H. Itoh, Spin injection into ferromagnetic metal from heavy metal owing to spin Hall effect, *Science and Technology Reports of Kansai University*, **64**, 51 (2022).

* Correspondence to: Syuta Honda, Department of Pure and Applied Physics, Kansai University, Suita, Osaka 564-8680, Japan. E-mail: shonda@kansai-u.ac.jp